

Orbital-dependent electron correlation in LiFeAs revealed by angle-resolved photoemission spectroscopy

T. Hajiri,^{1,2,*} T. Ito,^{1,3} M. Matsunami,^{2,4,†} B. H. Min,⁵ Y. S. Kwon,^{5,6} K. Kuroki,⁷ and S. Kimura^{2,7,8}

¹Graduate School of Engineering, Nagoya University, Nagoya 464-8603, Japan

²UVSOR Facility, Institute for Molecular Science, Okazaki 444-8585, Japan

³Nagoya University Synchrotron Radiation Research Center, Nagoya University, Nagoya 464-8603, Japan

⁴School of Physical Sciences, The Graduate University for Advanced Studies (SOKENDAI), Okazaki 444-8585, Japan

⁵DGIST-LBNL Joint Research Center, DGIST, Daegu 711-873, Republic of Korea

⁶Department of Emerging Materials Science, DGIST, Daegu 711-873, Republic of Korea

⁷Department of Physics, Graduate School of Science, Osaka University, Osaka 565-0043, Japan

⁸Graduate School of Frontier Biosciences, Osaka University, Suita 565-0871, Japan

(Received 12 February 2015; revised manuscript received 4 September 2015; published 6 January 2016)

We report on the electronic structure of the 111-type iron pnictide superconductor LiFeAs as a function of temperature using angle-resolved photoemission spectroscopy. Below approximately 50 K, both the d_{yz} hole band at the Z point and the $d_{xz/yz}$ electron band at the A point shift to a higher binding energy side. However, at the high-symmetry points Z , A , Γ , and M , the remaining bands are almost independent of temperature. One of the possible scenarios for these observations is that a strong, three-dimensional orbital-dependent correlation exists in the normal state of LiFeAs in relation to short-range spin fluctuations.

DOI: [10.1103/PhysRevB.93.024503](https://doi.org/10.1103/PhysRevB.93.024503)

I. INTRODUCTION

Iron pnictide superconductors [1], especially from the family of BaFe_2As_2 (namely, 122 type), exhibit a characteristic change in electronic structure even above T_c . For instance, $\text{BaFe}_2(\text{As}_{1-x}\text{P}_x)_2$ and $\text{Ba}(\text{Fe}_{1-x}\text{Co}_x)_2\text{As}_2$ systems have a fourfold rotational symmetry-broken phase (namely, the nematic phase) [2,3] above the temperature T of the spin-density-wave (SDW)/antiferromagnetic (AFM) and structural transitions [4–6]. The nematic phase is considered to be at the origin of anomalous physical properties, such as in-plane anisotropic resistivity [7], the softening of the C_{66} mode [8], the orbital-polarized electronic structure between d_{xz} and d_{yz} orbitals [9], and the pseudogap [10]. In addition, in $\text{Ba}(\text{Fe}_{1-x}\text{Co}_x)_2\text{As}_2$ systems, all bands shift with decreasing temperature due to thermally excited carriers in the narrow bands near the Fermi level E_F . It is considered that the band shift of $\text{Ba}(\text{Fe}_{1-x}\text{Co}_x)_2\text{As}_2$ systems is related to the temperature evolution of interband charge or spin fluctuations [11]. Because the electronic structure and physical properties above T_c are considered to be closely related to superconductivity, the electronic structure above T_c should be investigated to elucidate the origin of superconductivity in iron pnictides.

The 111-type iron pnictide superconductor LiFeAs is an ideal system for investigating the electronic structure above and below T_c , because stoichiometric LiFeAs shows superconductivity without SDW/AFM and structural transitions, which distinguishes it from other iron pnictides such as the 122 type. Previously, a spin-fluctuation scenario has been proposed for the superconductivity of LiFeAs [12–17]. However, no

orbital order/fluctuation behavior is observed in LiFeAs, in contrast to the case for the 122 type. The importance of orbital fluctuation for superconductivity is highlighted by a recent angle-resolved photoemission spectroscopy (ARPES) study [18] and by theoretical studies [19,20]. On the other hand, a possible new superconductivity mechanism has been reported for KFe_2As_2 , in which different effective interactions occur in the individual Fermi surfaces (FSs) [21]. In LiFeAs, the effective interactions in each FS are not yet clarified. Therefore, understanding the origin of superconductivity in iron pnictides requires elucidating the FS-dependent interactions and electronic structure above T_c in these materials.

In this paper, we thus report on the temperature-dependent electronic structure of LiFeAs. We found that the binding energies of both the d_{yz} hole band at the Z point and the $d_{xz/yz}$ electron band at the A point increase below $T \sim 50$ K, which is the temperature of the appearance of a spin fluctuation and is greater than T_c . The remaining bands are almost temperature independent. These results possibly suggest that a strong orbital-dependent correlation exists in the normal state in LiFeAs, which may be related to short-range spin fluctuations.

II. EXPERIMENT

Three-dimensional (3D) ARPES experiments were performed on single crystals of stoichiometric LiFeAs with approximately $T_{c,\text{onset}} = 19.7$ K [22]. ARPES measurements were performed at the SAMRAI end station of the undulator beamline 7U of UVSOR-III at the Institute for Molecular Science, Japan, using an MBS A-1 analyzer [23]. The energy and angular resolutions were approximately 8 meV and 0.17° , respectively. All measurements were performed on *in situ* cleaved samples in an ultrahigh vacuum under 1×10^{-8} Pa. We use the same inner potential (15.4 eV) and photon energies (which correspond to the high-symmetry points) as in our

*Present address: Department of Crystalline Materials science, Nagoya University, Nagoya 464-8603, Japan; t.hajiri@numse.nagoya-u.ac.jp

†Present address: Toyota Technological Institute, Nagoya 468-8511, Japan.

previous study [12]. E_F of the samples was determined with respect to that of an evaporated gold film.

III. RESULTS AND DISCUSSION

Figures 1(a)–1(d) show ARPES images at the Γ ($h\nu = 23$ eV) and Z ($h\nu = 35$ eV) points along the Γ - M and Z - A directions at $T = 100$ and 12 K, respectively. Two hole bands appear at both the Γ and Z points because of S polarization, which contrasts with previous studies that report three hole bands at the Γ point [12,13,24]. The use of S polarization prevents the innermost hole band at the Γ point from being clearly recognized in Fig. 1. The band detected by P polarization is shown in Supplemental Fig. S1 [25]. The observed inner and outer hole bands are attributed to d_{yz} and d_{xy} orbitals, respectively [12]. Figures 1(e) and 1(f) compare the dispersion of each band at $T = 100$ and 12 K

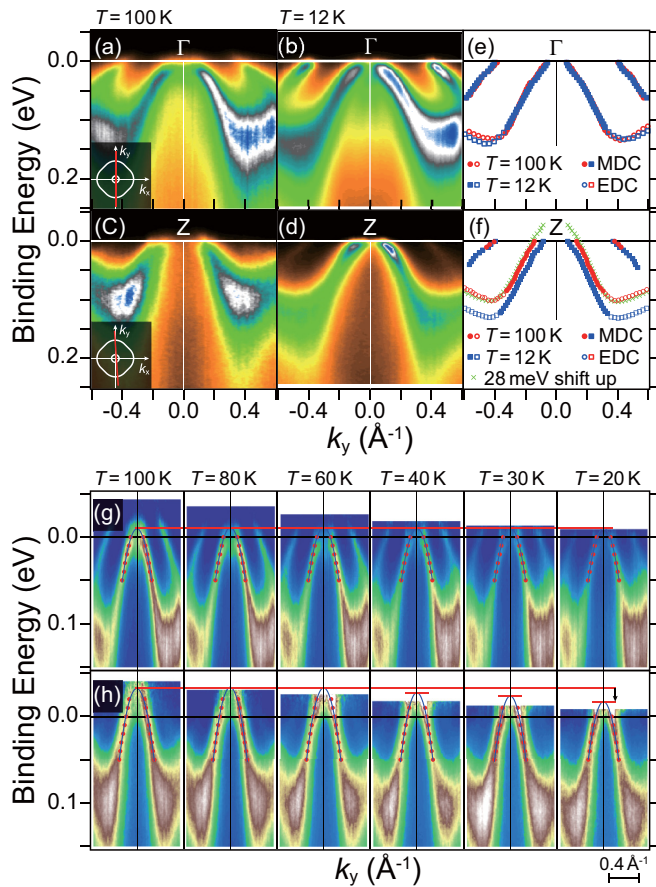


FIG. 1. (a)–(d) ARPES images along the Γ - M and Z - A directions obtained by S polarization at Γ ($h\nu = 23$ eV) and Z ($h\nu = 35$ eV) points at $T = 100$ and 12 K, respectively. The insets in (a) and (c) indicate the schematic FSs and measured momentum lines. (e), (f) Comparison of each band dispersion at the Γ and Z points between $T = 100$ and 12 K. The solid and open circles/squares show the peak positions of the MDCs and EDCs, respectively. The cross marks in (f) are the same as the inner hole band at $T = 12$ K after shifting up by 28 meV. (g), (h) Temperature-dependent ARPES images divided by the Fermi-Dirac function at the Γ and Z points. Solid circles and lines are the peak positions determined by the MDC fitting and its parabolic fitting, respectively.

at the Γ and Z points, respectively. The solid and open circles/squares in Figs. 1(e) and 1(f) were determined using the peak positions of the momentum-distribution curves (MDCs) and the energy-distribution curves (EDCs), respectively. At the Γ point shown in Fig. 1(e), the two observed bands do not shift with temperature. The innermost hole band attributed to the d_{xz} orbital seems to be almost independent of temperature, as shown in Supplemental Fig. S1 [25].

At the Z point shown in Fig. 1(f), however, the inner hole band attributed to the d_{yz} orbital rigidly shifts by 28 meV to higher binding energies with decreasing temperature, although the outer hole band is almost independent of temperature. To clarify the temperature-dependent band shift of the inner hole band, we show in Figs. 1(g) and 1(h) the temperature-dependent ARPES images divided by the Fermi-Dirac function at the Γ and Z points, respectively. The solid lines are determined by fitting the MDC peak positions to a parabola. Clearly, the top of the inner hole band at the Z point shifts below $T = 40$ K, but the inner hole band at the Γ point is independent of temperature. The Fermi wave vector k_F of the outer hole band at the Z point might shift slightly, but it can be negligible, as discussed in the Supplemental Material [25].

Next, we focus on the electron bands at the zone corner: the A and M points. Figures 2(a) and 2(b) show ARPES images at the A point ($h\nu = 18$ eV) along the Z - A direction at $T = 150$ and 15 K, respectively. As shown in Figs. 2(a2)–2(b3), which are second-derivative images of the EDCs [Figs. 2(a2) and 2(b2)] and MDCs [Figs. 2(a3) and 2(b3)] of the intensity images in Figs. 2(a1) and 2(b1), two electron bands centered at the A point appear at both temperatures. The deep and shallow electron bands are attributed to the d_{xy} and $d_{xz/yz}$ orbitals, respectively [12]. At $T = 150$ K, both electron bands have a similar k_F despite the different band bottoms at approximately 20 (shallow) and 90 (deep) meV. At $T = 15$ K, the bottom of the shallow electron band rigidly shifts to higher binding energies by approximately 20 meV, but the bottom of the deep electron band does not shift (see also Supplemental Fig. S4 [25]). Figure 2(c) shows the temperature dependence of the MDCs at E_F at the A point. The vertical lines indicate the k_F 's determined by Lorentzian fitting. Above $T = 80$ K, the shallow electron band has the same k_F as the deep band. At $T = 50$ K, a shoulder of the MDC at E_F , which originates from the shallow band, suddenly appears on the outer side of the main peak. On further decreasing the temperature, the shoulder structure shifts toward more outer wave vectors; this indicates that the bottom of the shallow electron band shifts toward higher binding energies.

To check the three-dimensionality of this temperature dependence of the band shift, we now turn our attention to the M point ($h\nu = 26$ eV) in the Γ - M direction. Figures 2(d) and 2(e) are ARPES images (lower panels) and MDCs at E_F (upper panels) at the M point at $T = 100$ and 20 K, respectively. Two electron bands across E_F and centered at the M point appear at both temperatures. In contrast to the A point, the k_F 's and the bottoms of both electron bands at 40 and 100 meV do not shift with temperature, as shown in Figs. 2(e) and 2(f). These results at the M and A points suggest that the shallower band at the A point shifts with decreasing temperature but that at the M point does not shift with temperature. These are the same relationships observed

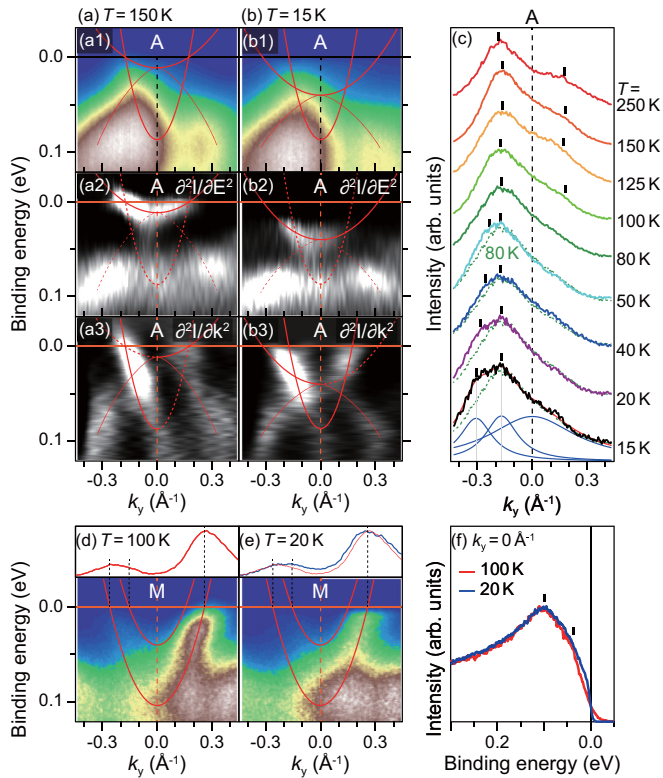


FIG. 2. (a), (b) ARPES results at the A point ($h\nu = 18$ eV) along the Z-A direction at $T = 150$ and 15 K, respectively. (a1), (b1) ARPES images; (a2), (b2) EDC's second-derivative images of (a1) and (b1), respectively; (a3), (b3) MDC's second-derivative images of (a1) and (b1), respectively. Electron bands are evaluated by a parabolic fitting of the EDC peak positions around the band bottoms and MDC peak positions around E_F . Hole bands are guides for the eyes. (c) The temperature-dependent MDCs at E_F at the A point. The vertical lines indicate the Fermi wave vectors obtained by the MDC fitting. MDC at 80 K is also plotted by a dashed line below 50 K as a guide. (d), (e) ARPES images (lower panels) and MDCs at E_F (upper panels) at the M point ($h\nu = 26$ eV) along the Γ -M direction at $T = 100$ and 20 K, respectively. (f) Comparison of EDCs at both temperatures at the M point.

between the inner hole band at the Z point and that at the Γ point.

Figure 3 summarizes the energy shifts of the top (bottom) of the hole (electron) bands at the Γ and Z (M and A) points as a function of temperature. The energies of the top (bottom) of the hole (electron) bands were evaluated by a parabolic fitting of the EDC/MDC and the EDC's/MDC's second-derivative peak position, as shown in Figs. 1 and 2. Figure 3(a) shows that the peak position of the Z point rapidly shifts below $T \sim 50$ K, which is approximately 2.5 times greater than T_c , in contrast to the lack of temperature dependence at the Γ point. At the M and A points [Fig. 3(b)], the shallow electron band around the A point also shifts below $T = 50$ K, but the deep electron band at the A point and the two electron bands at the M point are almost independent of temperature. It is noted that the reproducibility was checked by cleaving at both high (above 100 K) and low temperature (12 K). The shifted hole and electron bands are attributed

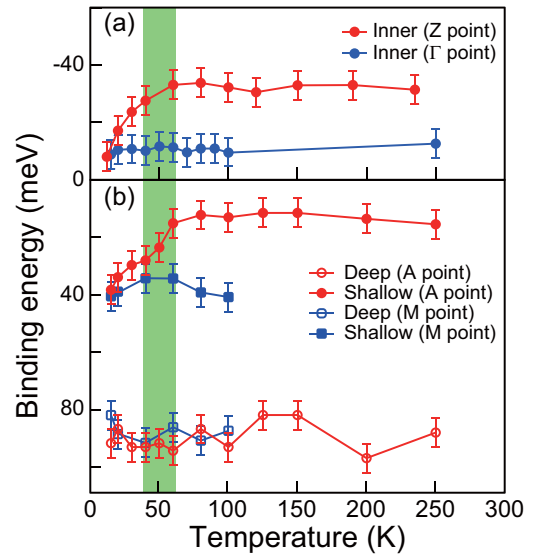


FIG. 3. (a) Temperature dependence of the top of the inner hole band at the Γ and Z points and (b) bottom of the electron bands at the M and A points.

to the d_{yz} and $d_{xz/yz}$ orbitals, respectively [12]. Therefore, our observations suggest that only the d_{xz} and d_{yz} orbitals exhibit an orbital-dependent electron correlation in LiFeAs. For 122-type $A\text{Fe}_{2-y}\text{Se}_2$ systems ($A = \text{K}, \text{Rb}$), only the d_{xy} orbital has been reported to have orbital-dependent electron correlations, but these systems have no temperature-dependent band shifts [26]. Therefore, the observations in our study differ completely from those of 122-type $A\text{Fe}_{2-y}\text{Se}_2$ systems.

To date, orbital ordering/fluctuations [9] and/or thermally excited carriers among the narrow bands [11] have been invoked to explain the temperature-dependent band shift in 122-type iron pnictide superconductors. However, in LiFeAs, neither the pseudogap nor the orbital-polarized electronic structure between the d_{xz} and d_{yz} orbitals at the M and A points are observed in our study; this suggests that the overall electronic structure in LiFeAs is not affected by orbital ordering/fluctuations. This is consistent with a recent scanning-tunneling-microscopy study in which LiFeAs does not have a symmetry-broken electronic structure, such as a 122-type nematic phase [27]. In addition, we observe that the narrow band at the Γ and M points does not shift but the narrow hole and electron bands at the Z and A points shift with temperature. The thermal excitation of carriers should be equivalent in a 3D momentum space; therefore, the temperature dependence of the band shift appears not to be due to the thermal excitation of carriers from the narrow bands.

Recently, a pseudogaplike feature below $T = 55$ K caused by antiferromagnetic fluctuations has been observed in ultrafast optical measurements for LiFeAs [28]. Indeed, the spin fluctuation is enhanced below $T \sim 50$ K [14,15]. This temperature of approximately 50 K is consistent with that of the observed band shift. This finding possibly suggests that the band shift is strongly related to spin fluctuations. In addition, in LiFeAs, a Lifshitz transition is observed in the hole FS with

only the d_{yz} orbital at the Z point and without the SDW/AFM transitions [29], possibly because of spin fluctuations [30].

Our observation might imply the violation of the Luttinger's theorem below $T = 50$ K (i.e., the hole concentration decreases, whereas the electron concentration increases). This feature is also observed in the normal state of NaFeAs, which is explained by short-range spin fluctuations [31] rather than a structural transition and/or fourfold-rotational-symmetry breaking [32]. An important difference between LiFeAs and NaFeAs is that, in the former, no structural transition exists (nor SDW). Thus, the one of the plausible explanations for the band shift is the existence of short-range spin fluctuations, as discussed in Ref. [31]. As stated in that study, fast probes such as ARPES are likely to capture the effect of short-range (local and fluctuating) ordering. In a previous study [31], band folding was observed, accompanied by a band shift, which is not observed in the present study. The intensity of the folded band in LiFeAs may be very weak as compared with that in NaFeAs; this may be due to the absence of SDW even at low temperatures. In LiFeAs, longitudinal magnetoresistance is observed below $T = 50$ K, which is similar to what happens in $\text{Ba}(\text{Fe}_{1-x}\text{Co}_x)_2\text{As}_2$ because of short-range spin fluctuations [33]. Therefore, one of the plausible interpretations for the selective band shift of LiFeAs below 50 K is accompanied by short-range spin fluctuations but with no SDW transition.

IV. CONCLUSION

To summarize, we performed ARPES measurements of the stoichiometric superconductor LiFeAs to clarify the temperature-dependent electronic structure at the high-symmetry points. The results show that the d_{yz} hole band at the Z point and the $d_{xz/yz}$ electron band at the A point shift to higher binding energies below approximately 50 K, whereas the other bands have almost no temperature dependence. These results might suggest that a strong 3D orbital-dependent correlation exists above T_c , possibly accompanied by short-range spin fluctuations.

ACKNOWLEDGMENTS

The authors gratefully acknowledge M. Sakai for his technical assistance during the experiments. Part of this work was supported by the Use-of-UVSOR Facility Program (BL7U, 2012, 2013) of the Institute for Molecular Science. The work at DGIST was partially supported by the Leading Foreign Research Institute Recruitment Program (Grant No. 2012K1A4A3053565) and Basic Science Research Program (NRF-2013R1A1A2009778) through the National Research Foundation of Korea funded by MEST. T.I. acknowledges support from Grant-in-Aid for Challenging Exploratory Research from JSPS (Grant No. 26610085). T.H. was supported by a Grant-in-Aid for JSPS Fellows (Grant No. 13J02477).

-
- [1] Y. Kamihara, T. Watanabe, M. Hirano, and H. Hosono, Iron-based layered superconductor $\text{La}[\text{O}_{1-x}\text{F}_x]\text{FeAs}$ ($x = 0.05\text{-}0.12$) with $T_c = 26$ K, *J. Am. Chem. Soc.* **130**, 3296 (2008).
- [2] S. Kasahara, H. J. Shi, K. Hashimoto, S. Tonegawa, Y. Mizukami, T. Shibauchi, K. Sugimoto, T. Fukuda, T. Terashima, A. H. Nevidomskyy, and Y. Matsuda, Electronic nematicity above the structural and superconducting transition in $\text{BaFe}_2(\text{As}_{1-x}\text{P}_x)_2$, *Nature (London)* **486**, 382 (2012).
- [3] T.-M. Chuang, M. P. Allan, J. Lee, Y. Xie, N. Ni, S. L. Bud'ko, G. S. Boebinger, P. C. Canfield, and J. C. Davis, Nematic electronic structure in the "parent" state of the iron-based superconductor $\text{Ca}(\text{Fe}_{1-x}\text{Co}_x)_2\text{As}_2$, *Science* **327**, 181 (2010).
- [4] W. Lv, J. Wu, and P. Phillips, Orbital ordering induces structural phase transition and the resistivity anomaly in iron pnictides, *Phys. Rev. B* **80**, 224506 (2009).
- [5] H. Kontani and S. Onari, Orbital-Fluctuation-Mediated Superconductivity in Iron Pnictides: Analysis of the Five-Orbital Hubbard-Holstein Mode, *Phys. Rev. Lett.* **104**, 157001 (2010).
- [6] Y. Yanagi, Y. Yamakawa, and Y. Ono, Two types of s -wave pairing due to magnetic and orbital fluctuations in the two-dimensional 16-band $d - p$ model for iron-based superconductors, *Phys. Rev. B* **81**, 054518 (2010).
- [7] M. Nakajima, S. Ishida, Y. Tomioka, K. Kihou, C. H. Lee, A. Iyo, T. Ito, T. Kakeshita, H. Eisaki, and S. Uchida, Effect of Co Doping on the In-Plane Anisotropy in the Optical Spectrum of Underdoped $\text{Ba}(\text{Fe}_{1-x}\text{Co}_x)_2\text{As}_2$, *Phys. Rev. Lett.* **109**, 217003 (2012).
- [8] M. Yoshizawa, D. Kimura, T. Chiba, S. Simayi, Y. Nakanishi, K. Kihou, C.-H. Lee, A. Iyo, H. Eisaki, M. Nakajima, and S. Uchida, Structural quantum criticality and superconductivity in iron-based superconductor $\text{Ba}(\text{Fe}_{1-x}\text{Co}_x)_2\text{As}_2$, *J. Phys. Soc. Jpn.* **81**, 024604 (2012).
- [9] M. Yi, D. Lu, J.-H. Chu, J. G. Analytis, A. P. Sorini, A. F. Kemper, B. Moritz, S.-K. Mo, R. G. Moore, M. Hashimoto, W.-S. Lee, Z. Hussain, T. P. Devereaux, I. R. Fisher, and Z.-X. Shen, Symmetry-breaking orbital anisotropy observed for detwinned $\text{Ba}(\text{Fe}_{1-x}\text{Co}_x)_2\text{As}_2$ above the spin density wave transition, *Proc. Natl. Acad. Sci. USA* **108**, 6878 (2011).
- [10] T. Shimojima, T. Sonobe, W. Malaeb, K. Shinada, A. Chainani, S. Shin, T. Yoshida, S. Ideta, A. Fujimori, H. Kumigashira, K. Ono, Y. Nakashima, H. Anzai, M. Arita, A. Ino, H. Namatame, M. Taniguchi, M. Nakajima, S. Uchida, Y. Tomioka, T. Ito, K. Kihou, C. H. Lee, A. Iyo, H. Eisaki, K. Ohgushi, S. Kasahara, T. Terashima, H. Ikeda, T. Shibauchi, Y. Matsuda, and K. Ishizaka, Pseudogap formation above the superconducting dome in iron pnictides, *Phys. Rev. B* **89**, 045101 (2014).
- [11] V. Brouet, P.-H. Lin, Y. Texier, J. Bobroff, A. Taleb-Ibrahimi, P. Le Fèvre, F. Bertran, M. Casula, P. Werner, S. Biermann, F. Rullier-Albenque, A. Forget, and D. Colson, Large Temperature Dependence of the Number of Carriers in Co-Doped BaFe_2As_2 , *Phys. Rev. Lett.* **110**, 167002 (2013).
- [12] T. Hajiri, T. Ito, R. Niwa, M. Matsunami, B. H. Min, Y. S. Kwon, and S. Kimura, Three-dimensional electronic structure and interband nesting in the stoichiometric superconductor LiFeAs, *Phys. Rev. B* **85**, 094509 (2012).
- [13] K. Umezawa, Y. Li, H. Miao, K. Nakayama, Z.-H. Liu, P. Richard, T. Sato, J. B. He, D.-M. Wang, G. F. Chen, H. Ding, T. Takahashi, and S.-C. Wang, Unconventional Anisotropic

- s*-Wave Superconducting Gaps of the LiFeAs Iron-Pnictide Superconductor, *Phys. Rev. Lett.* **108**, 037002 (2012).
- [14] L. Ma, J. Zhang, G. F. Chen, and W. Yu, NMR evidence of strongly correlated superconductivity in LiFeAs: Tuning toward a spin-density-wave ordering, *Phys. Rev. B* **82**, 180501(R) (2010).
- [15] Z. Li, Y. Ooe, X.-C. Wang, Q.-Q. Liu, C.-Q. Jin, M. Ichioka, and G.-q. Zheng, ^{75}As NQR and NMR studies of superconductivity and electron correlations in iron arsenide LiFeAs, *J. Phys. Soc. Jpn.* **79**, 083702 (2010).
- [16] A. E. Taylor, M. J. Pitcher, R. A. Ewings, T. G. Perring, S. J. Clarke, and A. T. Boothroyd, Antiferromagnetic spin fluctuations in LiFeAs observed by neutron scattering, *Phys. Rev. B* **83**, 220514(R) (2011).
- [17] S. Grothe, S. Chi, P. Dosanjh, R. Liang, W. N. Hardy, S. A. Burke, D. A. Bonn, and Y. Pennec, Bound states of defects in superconducting LiFeAs studied by scanning tunneling spectroscopy, *Phys. Rev. B* **86**, 174503 (2012).
- [18] S. V. Borisenko, V. B. Zabolotnyy, A. A. Kordyuk, D. V. Evtushinsky, T. K. Kim, I. V. Morozov, R. Follath, and B. Büchner, One-sign order parameter in iron based superconductor, *Symmetry* **4**, 251 (2012).
- [19] S. Onari, H. Kontani, S. V. Borisenko, V. B. Zabolotnyy, and B. Büchner, *S*-wave superconductivity due to orbital and spin fluctuations in Fe-pnictides: Self-consistent vertex correction with self-energy (SC-VCE) Analysis, [arXiv:1307.6119](https://arxiv.org/abs/1307.6119).
- [20] T. Saito, S. Onari, Y. Yamakawa, H. Kontani, S. V. Borisenko, and V. B. Zabolotnyy, Reproduction of experimental gap structure in LiFeAs based on orbital-spin fluctuation theory: s_{++} -wave, s_{\pm} -wave, and hole- s_{\pm} -wave states, *Phys. Rev. B* **90**, 035104 (2014).
- [21] K. Okazaki, Y. Ota, Y. Kotani, W. Malaeb, Y. Ishida, T. Shimojima, T. Kiss, S. Watanabe, C.-T. Chen, K. Kihou, C.-H. Lee, A. Iyo, H. Eisaki, T. Saito, H. Fukazawa, Y. Kohori, K. Hashimoto, T. Shibauchi, Y. Matsuda, H. Ikeda, H. Miyahara, R. Arita, A. Chainani, and S. Shin, Octet-line node structure of superconducting order parameter in KFe_2As_2 , *Science* **337**, 1314 (2012).
- [22] Y. J. Song, J. S. Ghim, B. H. Min, Y. S. Kwon, M. H. Jung, and J.-S. Rhyee, Synthesis, anisotropy, and superconducting properties of LiFeAs single crystal, *Appl. Phys. Lett.* **96**, 212508 (2010).
- [23] S. Kimura, T. Ito, M. Sakai, E. Nakamura, N. Kondo, T. Horigome, K. Hayashi, M. Hosaka, M. Katoh, T. Goto, T. Ejima, and K. Soda, SAMRAI: A novel variably polarized angle-resolved photoemission beamline in the VUV region at UVSOR-II, *Rev. Sci. Instrum.* **81**, 053104 (2010).
- [24] S. V. Borisenko, V. B. Zabolotnyy, D. V. Evtushinsky, T. K. Kim, I. V. Morozov, A. N. Yaresko, A. A. Kordyuk, G. Behr, A. Vasiliev, R. Follath, and B. Büchner, Superconductivity without Nesting in LiFeAs, *Phys. Rev. Lett.* **105**, 067002 (2010).
- [25] See Supplemental Material at <http://link.aps.org/supplemental/10.1103/PhysRevB.93.024503> for the details regarding the innermost hole band at the Γ point, the temperature dependence at the Z, and the EDC at the A point.
- [26] M. Yi, D. H. Lu, R. Yu, S. C. Riggs, J.-H. Chu, B. Lv, Z. K. Liu, M. Lu, Y.-T. Cui, M. Hashimoto, S.-K. Mo, Z. Hussain, C. W. Chu, I. R. Fisher, Q. Si, and Z.-X. Shen, Observation of Temperature-Induced Crossover to an Orbital-Selective Mott Phase in $A_x\text{Fe}_{2-y}\text{Se}_2$ ($A=\text{K, Rb}$) Superconductors, *Phys. Rev. Lett.* **110**, 067003 (2013).
- [27] E. P. Rosenthal, E. F. Andrade, C. J. Arguello, R. M. Fernandes, L. Y. Xing, X. C. Wang, C. Q. Jin, A. J. Millis, and A. N. Pasupathy, Visualization of electron nematicity and unidirectional antiferroic fluctuations at high temperatures in NaFeAs, *Nat. Phys.* **10**, 225 (2014).
- [28] K.-H. Lin, K.-J. Wang, C.-C. Chang, Y.-C. Wen, D.-H. Tsai, Y.-R. Wu, Y.-T. Hsieh, M.-J. Wang, B. Lv, P. C.-W. Chu, and M.-K. Wu, Observation of pseudogap-like feature above T_c in LiFeAs and $(\text{Ba}_{0.6}\text{K}_{0.4})\text{Fe}_2\text{As}_2$ by ultrafast optical measurement, [arXiv:1407.3539](https://arxiv.org/abs/1407.3539).
- [29] Z. R. Ye, Y. Zhang, F. Chen, M. Xu, J. Jiang, X. H. Niu, C. H. P. Wen, L. Y. Xing, X. C. Wang, C. Q. Jin, B. P. Xie, and D. L. Feng, Extraordinary Doping Effects on Quasiparticle Scattering and Bandwidth in Iron-Based Superconductors, *Phys. Rev. X* **4**, 031041 (2014).
- [30] C. Liu, T. Kondo, R. M. Fernandes, A. D. Palczewski, E. D. Mun, N. Ni, A. N. Thaler, A. Bostwick, E. Rotenberg, J. Schmalian, S. L. Bud'ko, P. C. Canfield, and A. Kaminski, Evidence for a Lifshitz transition in electron-doped iron arsenic superconductors at the onset of superconductivity, *Nat. Phys.* **6**, 419 (2010).
- [31] C. He, Y. Zhang, B. P. Xie, X. F. Wang, L. X. Yang, B. Zhou, F. Chen, M. Arita, K. Shimada, H. Namatame, M. Taniguchi, X. H. Chen, J. P. Hu, and D. L. Feng, Electronic-Structure-Driven Magnetic and Structure Transitions in Superconducting NaFeAs Single Crystals Measured by Angle-Resolved Photoemission Spectroscopy, *Phys. Rev. Lett.* **105**, 117002 (2010).
- [32] Y. Zhang, C. He, Z. R. Ye, J. Jiang, F. Chen, M. Xu, Q. Q. Ge, B. P. Xie, J. Wei, M. Aeschlimann, X. Y. Cui, M. Shi, J. P. Hu, and D. L. Feng, Symmetry breaking via orbital-dependent reconstruction of electronic structure in detwinned NaFeAs, *Phys. Rev. B* **85**, 085121 (2012).
- [33] F. Rullier-Albenque, D. Colson, and A. Forget, Longitudinal magnetoresistance in Co-doped BaFe_2As_2 and LiFeAs single crystals: Interplay between spin fluctuations and charge transport in iron pnictides, *Phys. Rev. B* **88**, 045105 (2013).